Normalization of Obesity-Associated Insulin Resistance through Immunotherapy: CD4+ T Cells Control Glucose Homeostasis

Shawn Winer[1,*], **Yin Chan**[1,*], **Geoffrey Paltser**[1], **Dorothy Truong**[1], **Hubert Tsui**[1], **Jasmine Bahrami**[2], **Ruslan Dorfman**[4], **Yongqian Wang**[4], **Julian Zielenski**[4], **Fabrizio Mastronardi**[1], **Yuko Maezawa**[1], **Daniel Drucker**[2], **Edgar Engleman**[3], **Daniel Winer**[3], and **H.-Michael Dosch**[1]

[1] Neuroscience & Mental Health program, Research Institute, The Hospital for Sick Children, University of Toronto Departments of Pediatrics & Immunology, 555 University Ave, Toronto, ON, Canada, M5G 1X8

[2] Department of Medicine, Samuel Lunenfeld Research Institute, Mount Sinai Hospital, University of Toronto, Toronto, ON, Canada

[3] Department of Pathology, Stanford University School of Medicine, Palo Alto, California, USA, 94304

[4] Program in Genetics and Genomic biology, Research Institute, The Hospital for Sick Children, University of Toronto

Abstract

Progressive obesity and its associated metabolic syndromes represent a globally growing challenge, yet mechanistic understanding and current therapeutics are unsatisfactory. We discovered that CD4+ T-lymphocytes, resident in visceral adipose tissue (VAT), control insulin-resistance in diet-induced obese (DIO) mice and likely humans. DIO VAT-associated T cells display biased TCR-Vα repertoires suggesting antigen-specific expansion. CD4+ T-lymphocyte control of glucose homeostasis is compromised in DIO when VAT accumulates pathogenic IFNγ-secreting Th1 cells, overwhelming static numbers of Th2 (CD4+GATA-3+) and regulatory Foxp3+ T cells. CD4+ T cell transfer into DIO, lymphocyte-free RAG[null] mice reversed weight gain and insulin resistance predominately through Th2 cells. Brief systemic treatment with αCD3 antibody or its F(ab′)$_2$ fragment, restores the Th1/Foxp3+ balance and reverses insulin resistance for months, despite continuing high-fat diet. The progression of obesity-associated metabolic abnormalities is physiologically under CD4+ T cell control, with expansion of adipose tissue-resident T cells that can be manipulated by immunotherapy.

Introduction

The incidence of obesity is increasing worldwide, its numerous consequences include a metabolic syndrome (MetSyn) of insulin-resistance, glucose-intolerance/toxicity, hepatic steatosis and dyslipidemia as well as the risk to develop Type 2 Diabetes (T2D). T2D and

[*]These authors contributed equally

obesity both involve genetic and environmental factors which represent a major global cause of morbidity and mortality, since current therapies are inadequate.

Together, the above elements contribute to persistent β-cell stress, dysfunction and T2D risk. However, progression of MetSyn to overt diabetes is not easily predicted, many patients with MetSyn never convert, some only transiently, and some obese individuals have only mild metabolic abnormalities while others progress to MetSyn,. Adipose tissue inflammation is viewed as a promoter of progression, but mechanisms remain unclear, as is the nature of what limits or halts progression in patients with persisting MetSyn or what drives T2D progression in converters.

Obesity-associated insulin-resistance is a core element of T2D development. The impairment of insulin-sensitivity involves multiple organs, prominently including growing adipose tissue with an associated rise in fatty acids, adipokines, and pro-inflammatory molecules such as IL-6 and TNFα,. TNFα can be produced by adipocytes, but overall, it is largely macrophage derived. Macrophages accumulate in both visceral and subcutaneous adipose tissue (VAT, SAT), playing distinct roles in obesity-induced insulin-resistance–.

Macrophage activation is modified by T-cells. IFNγ-secreting (Th1) as well as IL-17-secreting (Th17) T-cells enhance macrophage pro-inflammatory functions by inducing the release of IL-1, IL-6, and TNFα. In contrast, anti-inflammatory IL-4 and IL-13-secreting (Th2) as well as CD4+Foxp3+ T-cells regulate macrophage function by differentiating macrophages into anti-inflammatory IL-10 secreting, M2 or 'alternatively activated' macrophages (AAM),. AAM are characterized by abundant surface expression of macrophage mannose receptor (MMR) and intracellular arginase activity. Increased tissue levels of IL-10 improve insulin sensitivity in liver and fat, and AAM in adipose tissue have been demonstrated to normalize some of the metabolic abnormalities associated with diet-induced obesity in animal models,. Strategies increasing AAM or cells that induce them (e.g. Th2 or CD4+Foxp3+ T cells) might be of therapeutic promise in insulin resistance and T2D.

CD4+ and CD8+ T-cells enter VAT and SAT of obese mice and humans,. The function of these fat-associated T-cells (T^{fat}) and their conceivable roles in obesity and/or glucose homeostasis are unknown, nor are their antigen-specificities, activation history or T-sublineage profiles.

We investigated the impact of T-cells on the glucose homeostasis of C57BL/6 (B6) mice with diet-induced obesity (DIO). We discovered a progressive bias in the recruitment to and expansion of pro-inflammatory Th1 but not Th17 T-cells in adipose tissue, with a body mass-dependent, progressive paucity of CD4+Foxp3+ anti-inflammatory T-cells observed in obese mice and humans. We used independent experimental model systems in mice, to delineate several fat-resident immune elements with distinct impact on weight gain and/or insulin resistance and glucose homeostasis. Among these, the observation of T cell receptor bias in visceral fat was most unexpected, as it is typically associated with antigen specific T cell expansion and autoimmunity–.

The predominant T-cell effect on glucose homeostasis, revealed by T cell reconstitution studies in lymphocyte-free DIO RAG^{null} mice, was improvement of glucose tolerance,

enhanced insulin-sensitivity and lessening of weight gain. We identified the subsets involved and probed this T-cell potential with immunotherapy, utilizing the clinically effective αCD3 antibody and its non-mitogenic F(ab′)$_2$ fragment. Both αCD3 and F(ab′)$_2$ therapy dramatically normalized insulin resistance and glucose homeostasis, selectively restoring CD4+Foxp3+ T cell pools in VAT. Treatment was effective for months after a short course of injections, despite unchanged high-fat diet consumption. Fat-resident T lineage cells and their effects on local macrophages provide a physiological counter-regulation of inflammation-induced insulin resistance, which can be exploited therapeutically.

Results

Fat-resident T cells

We characterized numbers and subsets of T^{fat} from inguinal SAT and epididymal VAT of 14–18 week old high fat diet (HFD) and normal chow diet (NCD) fed B6 mice, consistently harvesting about 4×10^5 CD3+ T-cells/g VAT and SAT. The T^{fat} subset distribution varied somewhat, with a trend towards higher CD8:CD4 ratios in particular in VAT of HFD mice, compared to VAT of regular diet controls (Fig. 1a). VAT from lean and obese mice also contained pools of CD3+CD4/8 double-negative lymphocytes (i.e. NK, NKT, and Tγ/δ-lineage cells) and these were largely unaffected by obesity.

CD4+ effector T-cells can generally be sub-divided into pro-inflammatory Th1, Th17, and anti-inflammatory/regulatory Th2 and Foxp3+ sublineages. There were fewer IFNγ-secreting Th1 cells in SAT than in VAT from NCD and HFD B6 mice (Fig. 1b). HFD generated a strong IFNγ bias among T^{fat}, while it diminished the small VAT Th17 sublineage almost completely (Fig. 1b). Compared to VAT of regular diet mice, the proportion of anti-inflammatory CD4+Foxp3+ T cells in HFD VAT was reduced by 70%, likely contributing to the pro-inflammatory VAT profiles of obese mice (Fig. 1c). The ratio of Th1:Foxp3+ T cells in VAT increased from ~1.5:1 under regular diet to ~6.5:1 in DIO mice. In terms of absolute numbers, ~3 times more Th1 cells accumulate per gram of fat in HFD mice (Fig. 1d), while numbers of CD4+ Foxp3+ T cells/g of VAT vary little (Fig. 1d, lower right panel). The numbers of Th1 cells in adipose tissue represent the dynamic variable affected by diet induced obesity. The high proportions of CD4+Foxp3+ T cells in VAT of lean mice, progressively overwhelmed by IFNγ producers in DIO, suggested one candidate mechanism for worsening metabolic control (see below).

Observations in lean and obese humans were strikingly analogous. In VAT from obese humans (Fig. 1e, top right), Th1 cells that express the lineage-specific T-bet transcription factor (stained blue) outnumbered Foxp3+ T-cells ~12:1 (stained brown), while the ratio was ~6:1 in lean humans (Fig. 1e, bottom, see ratios in bottom left panel). The relative proportion of Th1 to Foxp3+ cells in VAT was correlated with body mass index (BMI) (Fig. 1e, top left panel, r^2=0.62). As in mice, human T^{fat} were observed clustered around blood vessels, some scattered between adipocytes (Fig. S1a). Foxp3+ T^{fat} were commonly observed in close proximity to monocytes/macrophages (Fig. S1b), predicting possible interactions with fat-associated monocytes/macrophages (see below).

Tissue-selective lymphocyte accumulation can reflect a number of mechanisms, including cognate events, involving T cell receptor engagements with its MHC:antigen complex. Although selective TCR engagement of VAT associated T cells was not expected, we decided to formally rule this possibility out, using ovalbumin (OVA) specific, 'OT2' TCR transgenics. These B6 mice develop metabolic complications of DIO (Fig. S2a–c). A small proportion of transgenic OT2 T cells can by-pass TCRα allelic exclusion and undergo random, secondary Vα-rearrangements, yielding a second surface TCR that can recognize non-OVA antigens. Such cells can be identified *via* reduced surface expression of the original, transgenic TCRVα, relative to CD3.

There were small pools (4–7%) of T cells with secondary TCRα rearrangements in spleens and SAT of HFD OT2 mice (Fig. 1f, boxes). Strikingly, secondary TCRα rearrangements in VAT were significantly and tissue selectively increased (8 to 21%), beginning at around 6 weeks of age (Fig. 1f) in mice on regular diet, but more so in HFD OT2 mice. This tissue-specific effect indicates strong selective pressure towards a non-OVA antigen(s), i.e. an adipose tissue antigen or antigen modification present only in VAT but not in SAT or elsewhere. Unexpectedly, T cell expansion in VAT appeared, at least in part, antigen-driven.

We sought further support for this notion and PCR amplified each of the 20 different TCRVα families in highly purified T cells with secondary TCRVα rearrangements. These cells had been sorted by FACS from spleens and VAT of obese, 16 week old OT2 mice, WT B6 spleens served as controls that expressed the expected, full spectrum of TCRα families (Fig. 1g). TCRVα's in spleen and VAT T cells from obese OT2 mice differed in TCRα-usage, only some were systemically shared, including the transgenic Vα-2. VAT T cells had lost Vα-3, but gained strong expression of Vα5 and Vα18. Spectra-typing of the CDR3 region in OT2 TCRα genes emphasized the strong selection pressures active in VAT, reducing systemic TCRVα's and generating impressive TCRVα bias among VAT T cells, including the unique Vα5 (417 base pairs) and Vα18 (393 bp) (Fig. S3).

Encouraged by the VAT tissue-specific TCR selection bias, and to rule out possible effects of the TCR transgene, we repeated this analysis but included sorted CD4+TCRβ+ NK1.1− VAT T cells from HFD as well as regular diet B6 WT mice (Fig. 1g, bottom two panels). Impressively, we observed a strong TCRVα bias in VAT of lean (10 of 20 TCRVα families expressed) and more so, HFD mice (only 7 of the 10 Vα-families used in lean mice) (Fig. 1g bottom panel). Spectratyping of the CDR3 region demonstrated dramatically altered diversity in VAT TCRVα repertoires of DIO *vs.* lean B6 mice (Fig. S4). These results suggest antigen specific expansion of T cell repertoires in VAT of lean mice, with increasing bias in obese mice, likely driven by adipose tissue changes that occur in obesity. Tissue-driven TCR bias is common in adaptive immunity and organ-selective autoimmune disorders–. However, this process has not previously been associated with obesity or T2D, and it will be rewarding to determine if it is indeed driven by tissue self-epitopes.

Metabolic role of T cells in obesity

HFD RAG[null] mice lack lymphocytes, gain more weight, and exhibit greater visceral adiposity than HFD WT mice (Fig. 2a, b). Increased visceral obesity in HFD-RAG[null] mice was mostly due to impressive adipocyte hypertrophy (Fig. 2c, and S5). There were no

significant abnormalities in body weight, adipose tissue mass nor adipocyte size in RAG[null] mice on regular diet (Fig. 2a–c), nor differences in food intake, CO_2 output or VO_2 consumption between HFD-RAG[null] and HFD-WT mice (Fig. 2d). Adipose tissue changes occur as a consequence of high fat intake and appeared to be limited in pathogenicity by lymphocytes.

Glucose and insulin tolerance in 14 week old, HFD-RAG[null] mice were severely impaired, with fasting glucose at diabetic levels (Fig. 2e, f), fasting hyperinsulinemia (Fig. 2f) and reduced insulin sensitivity upon insulin challenge (Fig. 2g). RAG[null] mice on regular diet showed non-significant trends towards poorer glucose tolerance and increased insulin resistance. However, a significant elevation of fasting blood glucose (Fig. 2e–g) implied that the metabolic role of lymphocytes may be physiological and revealed even in the absence of a hypercaloric diet.

CD4+ T cells regulate obesity and glucose homeostasis

The DIO RAG[null] phenotype delineated an overall protective role of lymphocytes in obesity and insulin resistance. To identify lymphocyte subsets involved in this process, we reconstituted 12 week old HFD-RAG[null] mice with 5×10^6 CD4+ or CD8+ T-cells, each specifically depleted of CD49b+ NK/NKT-cells, CD11b+ monocyte/macrophages and CD19+ and CD45R+ B-cells prior to transfer.

Two weeks following transfer, cells had populated spleen, SAT, and VAT with good purity (~95%, Fig. 3a). CD4+ (but not CD8+) T cell reconstitution reduced weight gain, quite notable by 2–4 weeks *post* transfer (Fig. 3b left panel), despite similar food intake, CO_2 output and O_2 consumption (Fig. S6a, b). Lesser weight gain reflected loss of SAT and even more so, VAT (Fig. 3b right panel), associated with reduced adipocyte size (Fig. 3c) compared to CD8+ T cell transferred HFD RAG[null] recipients or RAG[null] control mice (Fig. S5). CD4+ T cell transfer also reduced serum levels of obesity-associated adipokines, leptin, resistin and MCP-1 (Fig. S6c), normalized glucose tolerance, with lower fasting insulin and glucose levels, and improved insulin sensitivity within 2 weeks (Fig. 3d–f). CD4+ T cells, by themselves, have positive global impact on the panoply of DIO-induced metabolic derangements.

To determine the role of cognate, TCR-dependent events, we purified OVA-specific T cells from the OT2 TCR-transgenic B6 mouse by sorting cells without secondary rearrangements. Two weeks following adoptive transfer of these CD4+OT2:TCRVα[hi] lymphocytes into HFD RAG[null] mice, there were still almost no T cells with secondary rearrangements in spleens or fat (Fig. 3g). The presence of exclusively OVA-specific T cells in VAT failed to improve glucose tolerance (Fig. 3h), insulin sensitivity (Fig. 3i) fasting blood glucose (Fig. 3j left panel), fasting insulin levels (Fig. 3j middle panel), and body weight (Fig. 3j right panel). These results indicate that CD4+ T cells in VAT mediate the positive global controls of DIO-associated metabolic abnormalities in an antigen-specific fashion.

CD4+Foxp3+ T cells are regulators of inflammation, and CD4+ T cell transfer into HFD RAG[null] mice slowly re-populated RAG[null] VAT with CD4+Foxp3+ T cells, 2–3% by 2 weeks *post* transfer (Fig. 4a). To determine if CD4+Foxp3+ T cells were critical in the

regulation of glucose homeostasis following cell transfer, we sorted and transferred CD4+Foxp3− T cells, using the bi-cistronic, Foxp3-EGFP-transgenic B6 mouse line, where Foxp3+ cells co-express the fluorescent green marker.

Transferred Foxp3− CD4+ T cells showed little (~0.1%) conversion to CD4+Foxp3+ cells in spleen or VAT (Fig. 4a bottom), but recipient mice were as protected from weight gain as mice receiving full CD4+ T cell grafts from WT hosts (Fig. 4b). CD4+Foxp3− T cells were equally sufficient to improve glucose tolerance, fasting glucose and insulin levels (Fig. 4c, d), suggesting that metabolic control following CD4+ T cell transfer does not require CD4+Foxp3+ regulatory T cell function in the adoptive transfer model. Regulatory T cells and inducible type 1 regulatory T (Tr1) cells produce IL-10, a major anti-inflammatory cytokine as part of their effector function. Adoptive transfer of CD4+ T cells from IL-10^{null} B6 mice was as protective as full WT CD4+ grafts, indicating that T cell-derived IL-10 is dispensable for the beneficial effects of CD4+ T cells (Fig. 4b–d).

T cells can acquire a Th2 profile during the massive homeostatic expansion *post* transfer and we observed, for the first time, considerable Th2 cytokine production (IL-4 and IL-13) in VAT-derived T cells of HFD RAG^{null} CD4+ T cell recipients (Fig. 4e). Maintenance of Th2 cells is largely dependent on STAT6 and STAT6 deficiency severely impairs, but does not absolutely abrogate the Th2 sublineage, which can be identified by the GATA-3 transcription factor−. To determine the role of Th2 cells in our transfer model, we transferred CD4+STAT6^{null} T cells into HFD RAG^{null} mice. As expected, recipients of CD4+STAT6^{null} T cells displayed reduced numbers of CD4+GATA-3+ (Th2) T cells in VAT compared to those receiving WT CD4+ T cells (Fig. 4f). CD4+STAT6^{null} T cells lacked most of the positive CD4+ impact on glucose tolerance, fasting glucose, fasting insulin and weight gain, implicating metabolic functions for Th2 cells in the CD4+ T cell transfer model (Fig. 4g, h).

Implication of Th2 cells as regulators of glucose homeostasis in the transfer model prompted the characterization of this subset in VAT of regular diet and HFD WT mice (Fig. 4i, j). The proportions of Th2 (CD4+GATA-3+) cells were significantly reduced (~50%) in VAT of HFD mice (Fig. 4i, j left panel), however, the absolute numbers of Th2 cells/gram of VAT remained fairly constant (Fig. 4j right panel). As is the case with CD4+Foxp3+ T cells, reduced Th2 cell proportions in DIO VAT represent a candidate mechanism for worsening metabolic control in obese mice, and strategies which increase VAT Th2 cell content might be of therapeutic benefit.

Immunotherapy of insulin resistance

The various DIO-associated metabolic parameters relevant here are complex and immune controls likely involve multiple levels and mechanisms. While the paucity of CD4+Foxp3+ T cells in DIO VAT implicated these cells, the adoptive transfer model did not. To gain more insight in this issue, we employed an immunotherapy strategy (*in vivo* αCD3) that is dependent on CD4+Foxp3+ T cells for its long term tolerogenic effects,.

We injected mitogenic αCD3 anti-T cell antibody (10μg/d/5d) into 14 week old HFD WT mice. This protocol promotes T cell self-tolerance through global, transient (≲3 weeks) T cell depletion, paralleled by a selective increase of CD4+Foxp3+ T cell pools in sites of

tissue inflammation,. Nine weeks after αCD3 treatment, HFD mice had near lean levels of CD4+Foxp3+ T cells in VAT (Fig. 5a). Treatment improved fasting glucose, insulin levels, and greatly improved glucose tolerance and insulin sensitivity (Fig. 5b–d). There was a transient weight loss, lasting 3–4 week after αCD3 injection (Fig. 5e, left panel). This was likely attributable to the *post*-activation cytokine storm, with TNFα a major mediator,, since difference in body weight, adipocyte hypertrophy, food intake or CO_2/O_2 production/ consumption disappeared over the following weeks (Fig. 5e, S6d). Normalizing αCD3-effects on insulin resistance and glucose tolerance emerged 3–4 weeks after injection and lasted the entire observation period (≧4 months, Fig S7a–d), despite continued exposure to the hypercaloric diet. A similar, but slightly less effective impact on metabolic parameters was observed following treatment of leptin deficient ob/ob mice with αCD3 (Fig. S7e–i). Reduced efficiency of αCD3 in ob/ob mice correlated with reduced restoration of Treg numbers in VAT (Fig S7e).

Adverse effects of cytokine storm limit the utility of intact αCD3 therapy. We therefore tested the non-mitogenic F(ab′)$_2$ fragment of αCD3. Injection of 150μg of F(ab′)$_2$/day over 5 days resulted in long term improvements of glucose tolerance, fasting glucose and insulin levels (Fig. 5f) without weight loss (Fig. 5g) in HFD mice. F(ab′)$_2$ treatment also restored CD4+Foxp3+ T cell numbers in VAT (Fig 5h). Notably, the IFNγ/Th1 bias and other VAT cytokines measured remained unchanged by F(ab′)$_2$ therapy (Fig 5i, j), again pointing to, but not proving,, that restoration of VAT regulatory T cells improves long term glucose and insulin homeostasis. This brief, relatively non-toxic treatment protocol could be considered for seriously insulin-resistant patients.

CD4+Foxp3+ T cells can induce M2 or alternatively activated macrophages (AAM), which secrete IL-10, and protect against insulin resistance. To determine whether the restoration of VAT regulatory T cells by αCD3 immunotherapy did, in fact, generate IL-10 secreting M2 macrophages, we established cytokine profiles of M2 macrophages, based on surface staining of MMR. We distinguish three F4/80+ macrophage populations in VAT of both HFD and regular mice: MMR⁻, MMR^{lo} and MMR^{hi} (Fig. 6a). Only MMR^{hi} macrophages expressed IL-10, MMR^{lo} macrophages were the largest source of MCP-1, and MMR⁻ macrophages express MCP-1 and TNFα, likely representing classical M1 macrophages (Fig. 6b).

Interestingly, diet had little effect on these cytokine patterns (Fig. 6b, lower panel). However, HFD mice generated more TNFα-secreting MMR⁻ macrophages and less IL-10-secreting MMR^{hi} macrophages (Fig. 6a). F(ab′)$_2$ therapy increased the MMR^{hi} pool and reduced the MMR⁻ pool by 6 weeks *post* treatment (Fig. 6c). This macrophage shift generated an ~300% increase in IL-10 production as measured in purified VAT macrophages from F(ab′)$_2$ treated DIO-mice (Fig 6d). F(ab′)$_2$ therapy appears to have dual functions, increasing both anti-inflammatory T cell and macrophage compartments in VAT.

Discussion

We identified a fundamental role for CD4+ T lymphocytes in the regulation of body weight, adipocyte hypertrophy, insulin-resistance and glucose tolerance, implicating these cells in

the control of disease progression in diet induced obesity. Lymphocyte impact was revealed using independent models and experiments, including RAG^{null} mice, which develop a frankly diabetic phenotype on a high fat diet.

Our evidence maps T cell-mediated metabolic rescue to both, CD4+Foxp3+ and CD4+Foxp3−, e.g. Th2, T-cell compartments. While CD4+Foxp3− cells impacted obesity and insulin resistance, effects of CD4+Foxp3+ cells primarily regulated insulin resistance, although this was not as apparent in transfer models. Th2 cells did emerge as a regulator of obesity and insulin resistance in the transfer model. Overall, our experiments do not rule out effects of B lymphocytes or VAT-associated innate lymphocyte subsets (e.g. NK/NKT, TCRγ/δ, CD4^{neg}CD8^{neg} TCRα/β+). In fact, our preliminary data suggest that B cell deficiency in DIO mice is associated with improved metabolic control (Winer, Chan et al., unpublished).

We primarily focused on mouse models, but limited human studies support conclusions derived from mouse experiments. VAT of DIO mice and obese humans are characterized by an abnormally high Th1:Foxp3 ratio; high expression of IFNγ in human VAT was previously associated with increased waist circumference. IFNγ is a pro-inflammatory cytokine and increased levels of Th1 cells in VAT may contribute to insulin resistance; an observation supported by improved glucose tolerance in Th1 cell deficient IL-12p35^{null} mice (Winer et al. unpublished observation) and IFNγ^{null} mice. We favor a model where a relatively constant pool of CD4+Foxp3+ and Th2 T^{fat} gradually fails to regulate expanding pools of Th1 cells, leading to a progressively pro-inflammatory environment that promotes insulin resistance. It is also possible that Treg function may be suboptimal in the inflammatory VAT environment, as suggested in autoimmune disease models. Factors that drive Th1 cell influx and/or expansion in VAT are unknown, but may include antigen-driven expansion and the Th1 chemokine, RANTES (CCL5).

The precise mechanisms by which CD4+ T-cells affect insulin-sensitivity require further study. The induction of IL-10-secreting M2 macrophages represents one potential mechanism. CD4+Foxp3+ T-cells induce M2c type AAMs through production of IL-10 and TGF-β, while Th2 T cells can induce M2a type AMMs. AAMs can regulate insulin resistance through production of IL-10–mediated reversal of TNFα-induced insulin resistance. AAMs are present in adipose tissue of lean mice, but as obesity ensues, there is a proportionate shift to pro-inflammatory M1 macrophages. This shift to M1 macrophages is likely a result of steadily increasing Th1:Foxp3 and Th1:Th2 ratios. In fact, we observed increases in VAT M2 macrophages and decreases in M1 macrophages following restoration of CD4+Foxp3+ T cell pools *post* F(ab′)$_2$ immunotherapy.

αCD3 is a potent, clinically used immunosuppressant, and a possible therapeutic in Type 1 Diabetes,. Its immune effects are reversible, well understood, monitored, and data presented here suggest that it may be of use in the treatment of severe insulin resistance. In such patients, use of αCD3 may have multiple benefits, as αCD3 is effective in reducing atherosclerotic plaques, common in obesity and insulin resistance syndromes. We observed a similar, but slightly less effective course of αCD3 immunotherapy in diabetic, leptin-deficient ob/ob mice. Leptin affects multiple pathways in the immune response, including

TGF-β signaling, T cell homeostasis and macrophage/dendritic cell maturation,. αCD3 immunotherapy requires TGF-β secretion by phagocytes and deficiencies in this pathway may account for reduced efficiency in leptin deficient mice.

Although we focused on the metabolic roles of lymphocytes in VAT, we cannot rule out lymphocyte impact on insulin resistance in other organs such as liver. We also cannot rule out a role for CD8+ T cells in disease development. Although transfer studies show that CD8 T cells by themselves likely play little role in obesity and associated insulin resistance, it is possible that with CD4+ T cell help, CD8+ T cells and possibly even the regulatory CD8+ subsets become more active participants.

Our perhaps most surprising observation was the discovery of TCRVα bias in DIO OT2 and B6 mice. Antigen-driven T cell selection and expansion in VAT would be the most likely explanation, supported by the failure of exclusively OVA-specific T cells to transfer the panoply of metabolic, ultimately protective T cell functions. Further validation, through identification of candidate adipose tissue epitopes, would imply autoimmunity in obesity, despite minimal tissue destruction and absent autoimmune *disease*.

Collectively, we have demonstrated a new, previously unknown role for the adaptive immune system in the regulation of obesity, fat distribution and insulin-resistance. Our observations identify several T cell populations as physiological regulators in these processes and they demonstrate VAT-selective, TCR-dependent, cognate immunity as one element driving T cell expansion in VAT. This observation strongly implies that VAT incites active T cell immunity. Ultimately, we must identify inciting antigenic epitopes to open diet induced obesity and, possibly T2D, with their associated metabolic syndromes, to globally affordable tolerogenic vaccination strategies.

Methods

Mice

WT C57BL/6 mice, ob/ob, RAG[null], IL-10[null], STAT[null], Foxp3-EGFP, and OT2 mice were purchased from Jackson Laboratories (http://www.jax.org/) and maintained in our vivarium in a pathogen-free, temperature controlled, 12 hr light and dark cycle environment. Animals received either NCD or HFD (Research Diets Inc, 60 kcal% fat, from 6 wk of age on). All studies used males under approved protocols and in agreement with animal ethics guidelines.

Cell transfer experiments

Splenocytes from 8 wk old B6 NCD mice were isolated as described and CD4+ and CD8+ T-cells were purified (>95%, Easy Sep, StemCell Technologies Inc). 12wk old HFD-RAG[null] mice received 5×10^6 T-cells i.p.

Diet and metabolic studies

All WT and knock-out DIO males were weighed regularly. After 8 wk on HFD, fasting blood sugars and insulin levels were measured (Crystal Chem Inc ELISA). For GTT, fasted (16hr) mice received 0.75–1 g/kg glucose, for ITT mice received 0.75 U/kg of human

regular insulin (Eli Lilly) (2U/kg in ob/ob). For VAT:SAT ratios, weights of epididymal (VAT) and inguinal (SAT) fat pads were pooled and averaged. Fat cell diameter was measured using the straight-line tool in Image SXM software. At least 200 fat cells taken from 2 different sections of tissue were quantified for each mouse.

Oxymax and food intake studies

Mice were placed in individual metabolic chambers with free access to water and pre-weighed food. Oxygen consumption, CO_2 output, and heat were measured at 15 min intervals over 22 hours by indirect calorimetry (Oxymax System, Columbus Instruments). All measurements were normalized to body weight. Food intake was measured by food weights. Studies comparing DIO-WT and DIO–RAG[null] mice were performed at Jackson Laboratories.

T[fat] isolation

Anesthetized mice (isoflurane) were systemically perfused (PBS). Epididymal VAT and inguinal SAT pads were dissected, avoiding lymph nodes, mashed and digested in collagenase (0.2 mg/ml, DMEM/45′/37°C, manual shaking q5min, Sigma). Cells were washed, pelleted and filtered through a 40 μm filter to obtain stromal vascular cells (SVC) containing T[fat].

Flow cytometry and ELISAs

Splenocytes and/or T[fat] were stained (30 min) with the following antibody dilutions: CD3 (1/150), CD4 (1/200), IL-17 (1/150), IFNγ (1/100), FOXP3 (1/100), IL-10 (1/100) (eBioscience), GATA-3 (pre-diluted), CD8 (1/300) (BD Bioscience). Macrophages were stained with F4/80-PE (1/100) (eBioscience) and sorted. MMR staining utilized APC-streptavidin (1:100) (eBioscience) and biotinylated-MMR (1/50) (R&D systems). Anti-OT2 TCR heavy and light chain antibodies (1/100) were a gift by Dr. Dana Philpott (University of Toronto). For intracellular staining of T cells, cells were incubated with PMA (50 ng/ml) and ionomycin (750 ng/ml) for 14 hr in HL-1 media at 37°C and golgi blocked with Golgistop (BD Bioscience) for the last 11 hr. All FACS plots were analyzed using Flowjo software.

Serum levels of TNF-α, IL-6, adiponectin, leptin, and resistin were blindly measured by ELISA (AssayGate Inc). T[fat] ($200×10^3$) were isolated as above and stimulated with plate bound anti-CD3 (1 μg/ml) and anti-CD28 (0.25 μg/ml) for 72 hr in HL-1 media (Lonza). F4/80+ macrophages ($150×10^3$) were sorted from adipose SVC and stimulated with LPS (100 ng/mL, 24hr, 10% FBS/HL-1 media). For macrophage subset-studies, 10^5/macrophage subset were stimulated *ex vivo*. All ELISAs followed manufacturer's protocols: IFNγ, IL-10, IL-4 (BD Bioscience), IL-17, IL-13 (R&D systems) MCP-1, TNF-α (eBioscience).

Anti-CD3

10 μg anti-CD3 (clone 145-2C11 BD Biosciences) or purified hamster IgG isotype control (eBioscience) were injected i.p./100 μl PBS/5 consecutive days. For F(ab′)$_2$ experiments, 150 μg of F(ab′)$_2$ (Bio X Cell) or isotype (Bio X Cell) were injected i.p./150 μl of PBS/5 consecutive days.

Histology, Immunohistochemistry

VAT and SAT fat pads were fixed (24hr, 10% buffered formalin). H&E stains were analyzed blindly by 2 people, including one certified pathologist (D.W.). Human VAT was obtained from mesenteric fat of surgically removed colons from colon cancer patients. All studies involving human tissue was reviewed and approved in accordance with guidelines set by the Stanford Internal Review Board for Human Subjects. Immunohistochemistry used paraffin sections subjected to antigen retrieval in pH 6 Diva Decloaker (Biocare Medical) with the following antibody dilutions: 1/100 mouse anti-FOXP3 (Abcam), 1/100 rabbit anti-T-bet (Santa Cruz), 1/100 rabbit anti-CD14 (Atlas). Color was developed (DAB, Vector labs, Ferangi blue, Biocare Medical). T-bet:Foxp3 ratios were obtained by counting at least 200 stained cells from 2 different levels of tissue. There was no tumor infiltration in the areas examined.

TCR studies

The following cells were FACS sorted into RNALater stabilization reagent (Qiagen): ~100,000 splenic- and ~10,000 VAT-derived rearranged OT2 T-cells (CD4$^+$ Tg TCR Vα^{lo}) from pooled DIO OT2 mice (n=5; 16 wk old); ~5×10^6 splenic- and ~50,000 VAT-derived WT T-cells (CD4$^+$ TCR Vβ^+ NK1.1^{neg}) from pooled DIO B6 mice (n=10; 16 weeks of age) and regular B6 mice (n=18; 16 weeks of age). RNA was extracted using RNA Mini kit (Qiagen) and cDNA was prepared by random priming (Qiagen).

Nested-amplification of TCRα gene cDNAs employed two sets of nascent degenerate sense variable region primers (Vα1-Vα20) and anti-sense primers in the constant region as described. PCR products from the 2nd amplification round were analyzed on E-Gel® pre-cast Agarose Electrophoresis System (Invitrogen). For high-resolution analysis, OT2 2nd round products, generated with 5$'$-FAM-labeled constant region primers, were run on a ABI Prism 3100 Genetic Analyser and analyzed using GeneScan software v3.7.

Statistical analysis

Statistical significance between two means was assessed by Mann-Whitney and unpaired t-tests. Welch correction on t-tests was employed for sample sizes <6. Analysis of curves was performed using Two-Way ANOVA. Statistical significance was two tailed and set at 5%.

Supplementary Material

Refer to Web version on PubMed Central for supplementary material.

Acknowledgments

References

1. Kahn SE, Hull RL, Utzschneider KM. Mechanisms linking obesity to insulin resistance and type 2 diabetes. Nature. 2006; 444:840–846. [PubMed: 17167471]

2. Despres JP, Lemieux I. Abdominal obesity and metabolic syndrome. Nature. 2006; 444:881–887. [PubMed: 17167477]

3. Dahabreh IJ. Meta-analysis of rare events: an update and sensitivity analysis of cardiovascular events in randomized trials of rosiglitazone. Clin Trials. 2008; 5:116–120. [PubMed: 18375649]

4. Hanson RL, Imperatore G, Bennett PH, Knowler WC. Components of the "metabolic syndrome" and incidence of type 2 diabetes. Diabetes. 2002; 51:3120–3127. [PubMed: 12351457]

5. Hotamisligil GS. Inflammation and metabolic disorders. Nature. 2006; 444:860–867. [PubMed: 17167474]

6. Kanda H, et al. MCP-1 contributes to macrophage infiltration into adipose tissue, insulin resistance, and hepatic steatosis in obesity. J Clin Invest. 2006; 116:1494–1505. [PubMed: 16691291]

7. Yuan M, et al. Reversal of obesity- and diet-induced insulin resistance with salicylates or targeted disruption of Ikkbeta. Science. 2001; 293:1673–1677. [PubMed: 11533494]

8. Weisberg SP, et al. CCR2 modulates inflammatory and metabolic effects of high-fat feeding. J Clin Invest. 2006; 116:115–124. [PubMed: 16341265]

9. Odegaard JI, et al. Macrophage-specific PPARgamma controls alternative activation and improves insulin resistance. Nature. 2007; 447:1116–1120. [PubMed: 17515919]

10. Tiemessen MM, et al. CD4+CD25+Foxp3+ regulatory T cells induce alternative activation of human monocytes/macrophages. Proc Natl Acad Sci U S A. 2007; 104:19446–19451. [PubMed: 18042719]

11. Martinez FO, Sica A, Mantovani A, Locati M. Macrophage activation and polarization. Front Biosci. 2008; 13:453–461. [PubMed: 17981560]

12. Cintra DE, et al. Interleukin-10 is a protective factor against diet-induced insulin resistance in liver. J Hepatol. 2008; 48:628–637. [PubMed: 18267346]

13. Lumeng CN, Bodzin JL, Saltiel AR. Obesity induces a phenotypic switch in adipose tissue macrophage polarization. J Clin Invest. 2007; 117:175–184. [PubMed: 17200717]

14. Rausch ME, Weisberg S, Vardhana P, Tortoriello DV. Obesity in C57BL/6J mice is characterized by adipose tissue hypoxia and cytotoxic T-cell infiltration. Int J Obes (Lond). 2007

15. Kintscher U, et al. T-lymphocyte Infiltration in Visceral Adipose Tissue. A Primary Event in Adipose Tissue Inflammation and the Development of Obesity-Mediated Insulin Resistance. Arterioscler Thromb Vasc Biol. 2008

16. Wu H, et al. T-cell accumulation and regulated on activation, normal T cell expressed and secreted upregulation in adipose tissue in obesity. Circulation. 2007; 115:1029–1038. [PubMed: 17296858]

17. Baker FJ, Lee M, Chien YH, Davis MM. Restricted islet-cell reactive T cell repertoire of early pancreatic islet infiltrates in NOD mice. Proc Natl Acad Sci U S A. 2002; 99:9374–9379. [PubMed: 12082183]

18. Turner SJ, Doherty PC, McCluskey J, Rossjohn J. Structural determinants of T-cell receptor bias in immunity. Nat Rev Immunol. 2006; 6:883–894. [PubMed: 17110956]

19. Oksenberg JR, et al. Limited heterogeneity of rearranged T-cell receptor V alpha transcripts in brains of multiple sclerosis patients. Nature. 1990; 345:344–346. [PubMed: 1971424]

20. Jenkins RN, Nikaein A, Zimmermann A, Meek K, Lipsky PE. T cell receptor V beta gene bias in rheumatoid arthritis. J Clin Invest. 1993; 92:2688–2701. [PubMed: 8254025]

21. Belghith M, et al. TGF-beta-dependent mechanisms mediate restoration of self-tolerance induced by antibodies to CD3 in overt autoimmune diabetes. Nat Med. 2003; 9:1202–1208. [PubMed: 12937416]

22. Caspar-Bauguil S, et al. Adipose tissues as an ancestral immune organ: site-specific change in obesity. FEBS Lett. 2005; 579:3487–3492. [PubMed: 15953605]

23. Szabo SJ, et al. A novel transcription factor, T-bet, directs Th1 lineage commitment. Cell. 2000; 100:655–669. [PubMed: 10761931]

24. Barnden MJ, Allison J, Heath WR, Carbone FR. Defective TCR expression in transgenic mice constructed using cDNA-based alpha- and beta-chain genes under the control of heterologous regulatory elements. Immunol Cell Biol. 1998; 76:34–40. [PubMed: 9553774]

25. Padovan E, et al. Expression of two T cell receptor alpha chains: dual receptor T cells. Science. 1993; 262:422–424. [PubMed: 8211163]

26. Fontenot JD, Rasmussen JP, Gavin MA, Rudensky AY. A function for interleukin 2 in Foxp3-expressing regulatory T cells. Nat Immunol. 2005; 6:1142–1151. [PubMed: 16227984]

27. Awasthi A, et al. A dominant function for interleukin 27 in generating interleukin 10-producing anti-inflammatory T cells. Nat Immunol. 2007; 8:1380–1389. [PubMed: 17994022]

28. Jankovic D, et al. Single cell analysis reveals that IL-4 receptor/Stat6 signaling is not required for the in vivo or in vitro development of CD4+ lymphocytes with a Th2 cytokine profile. J Immunol. 2000; 164:3047–3055. [PubMed: 10706693]

29. Shimoda K, et al. Lack of IL-4-induced Th2 response and IgE class switching in mice with disrupted Stat6 gene. Nature. 1996; 380:630–633. [PubMed: 8602264]

30. Kaplan MH, Schindler U, Smiley ST, Grusby MJ. Stat6 is required for mediating responses to IL-4 and for development of Th2 cells. Immunity. 1996; 4:313–319. [PubMed: 8624821]

31. Bisikirska B, Colgan J, Luban J, Bluestone JA, Herold KC. TCR stimulation with modified anti-CD3 mAb expands CD8+ T cell population and induces CD8+CD25+ Tregs. J Clin Invest. 2005; 115:2904–2913. [PubMed: 16167085]

32. Chatenoud L, Bluestone JA. CD3-specific antibodies: a portal to the treatment of autoimmunity. Nat Rev Immunol. 2007; 7:622–632. [PubMed: 17641665]

33. Alegre M, et al. Acute toxicity of anti-CD3 monoclonal antibody in mice: a model for OKT3 first dose reactions. Transplant Proc. 1990; 22:1920–1921. [PubMed: 2143864]

34. Alegre M, et al. Hypothermia and hypoglycemia induced by anti-CD3 monoclonal antibody in mice: role of tumor necrosis factor. Eur J Immunol. 1990; 20:707–710. [PubMed: 2138564]

35. Zeyda M, Stulnig TM. Adipose tissue macrophages. Immunol Lett. 2007; 112:61–67. [PubMed: 17719095]

36. Rocha VZ, et al. Interferon-gamma, a Th1 cytokine, regulates fat inflammation: a role for adaptive immunity in obesity. Circ Res. 2008; 103:467–476. [PubMed: 18658050]

37. Korn T, et al. Myelin-specific regulatory T cells accumulate in the CNS but fail to control autoimmune inflammation. Nat Med. 2007; 13:423–431. [PubMed: 17384649]

38. Herold KC, et al. Anti-CD3 monoclonal antibody in new-onset type 1 diabetes mellitus. N Engl J Med. 2002; 346:1692–1698. [PubMed: 12037148]

39. Steffens S, Mach F. Adiponectin and adaptive immunity: linking the bridge from obesity to atherogenesis. Circ Res. 2008; 102:140–142. [PubMed: 18239140]

40. Macia L, et al. Impairment of dendritic cell functionality and steady-state number in obese mice. J Immunol. 2006; 177:5997–6006. [PubMed: 17056524]

41. Kumpers P, et al. Leptin is a coactivator of TGF-beta in unilateral ureteral obstructive kidney disease. Am J Physiol Renal Physiol. 2007; 293:F1355–1362. [PubMed: 17686962]

42. Perruche S, et al. CD3-specific antibody-induced immune tolerance involves transforming growth factor-beta from phagocytes digesting apoptotic T cells. Nat Med. 2008; 14:528–535. [PubMed: 18438416]

43. Winer S, et al. Autoimmune Islet Destruction in Spontaneous Type 1 Diabetes is not beta-Cell Exclusive. Nature Medicine. 2003; 9:198–205.
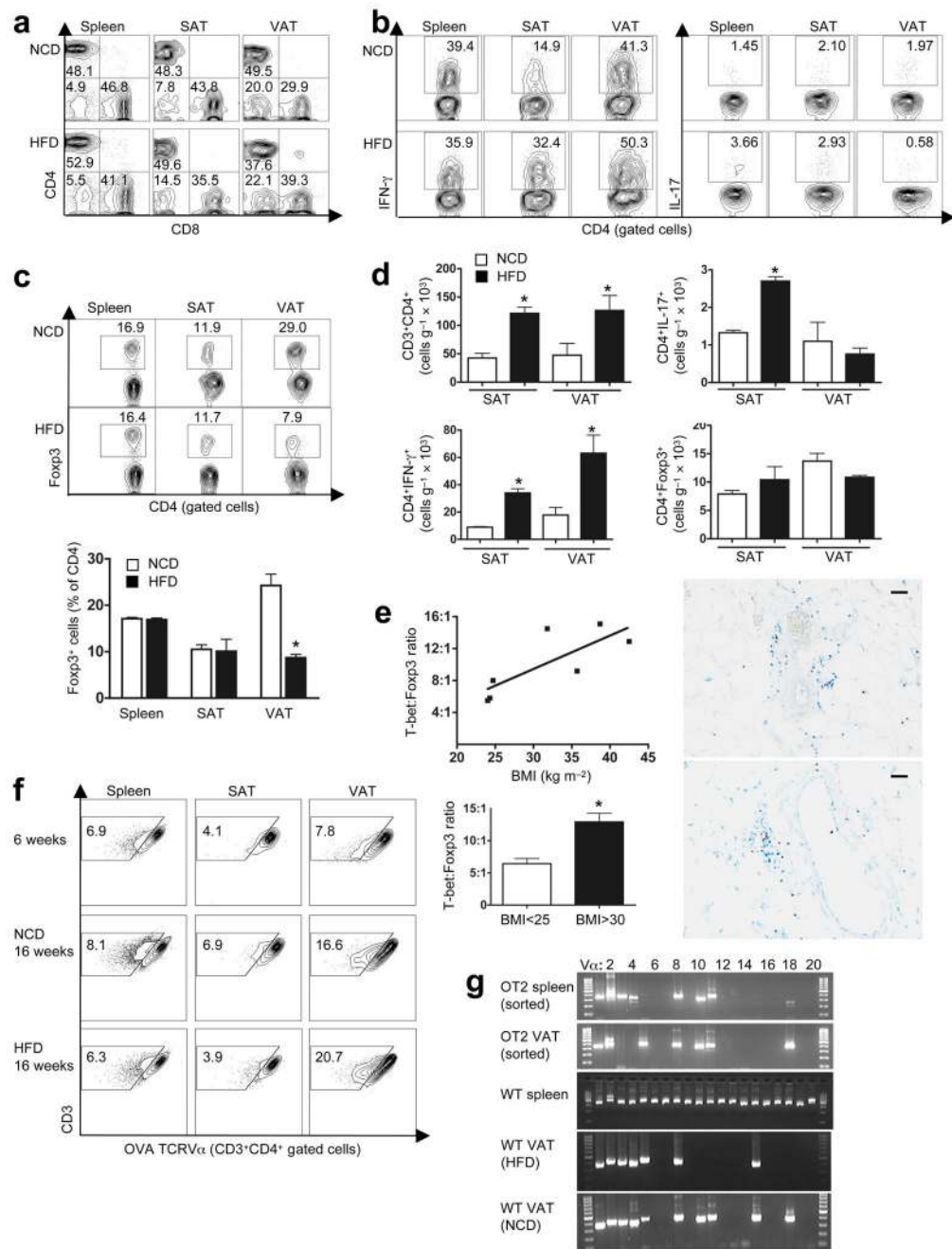
Figure 1. Phenotype of T^fat (all mice 14–16 wk old, each contour plot represents 3–4 independent experiments)

a) CD4 and CD8 expression on CD3+ cells in spleen and SAT and VAT of B6 high fat diet (HFD) and normal chow diet (NCD) mice. **b)** Proportion of CD4+IFNγ+ (Th1) and CD4+IL-17+ (Th17) T-cells in spleen, SAT and VAT. **c)** Proportion of CD4+Foxp3+ (Treg) cells in spleen, SAT and VAT (upper panel: FACS plots; lower panel: pooled data; *p<0.03, t-test). **d)** Total number of CD3+CD4+, CD4+IFNγ+ (Th1), CD4+IL-17+ (Th17), CD4+Foxp3+ (Treg) T cells/g of SAT and VAT in normal chow diet and HFD mice (n=4–5/ group, *p<0.05, t-test). **e)** T-bet (Th1):Foxp3 ratio in human VAT (upper left panel, r²=0.62,

p<0.05). Lower left panel: VAT T-bet:Foxp3 ratio in patients with BMI>30 *vs. <25* (*p<0.02, t-test). Upper right panel: Foxp3 (brown) and T-bet (blue, Th1 cells) in human VAT (BMI>30); lower right panel: BMI<25, bar 50 μm; T-bet:Foxp3 ratios from >200 stained cells/2 tissue levels. **f)** CD3+CD4+ T cells (%) with secondary re-rearranged. non-OVA TCRα detected by reduced OT2 TCRα:CD3 ratio in spleens, SAT and VAT of 6 or 16 wk old, regular diet or HFD B6 OT2 mice. **g)** TCRVα gene usage of CD4+ T cells isolated from spleens of 16 wk old obese wild type (WT) or OT2 mice, and from VAT of HFD and NCD WT and OT2 mice. CD4+ OT2 T cells were identified and sorted as in (f).
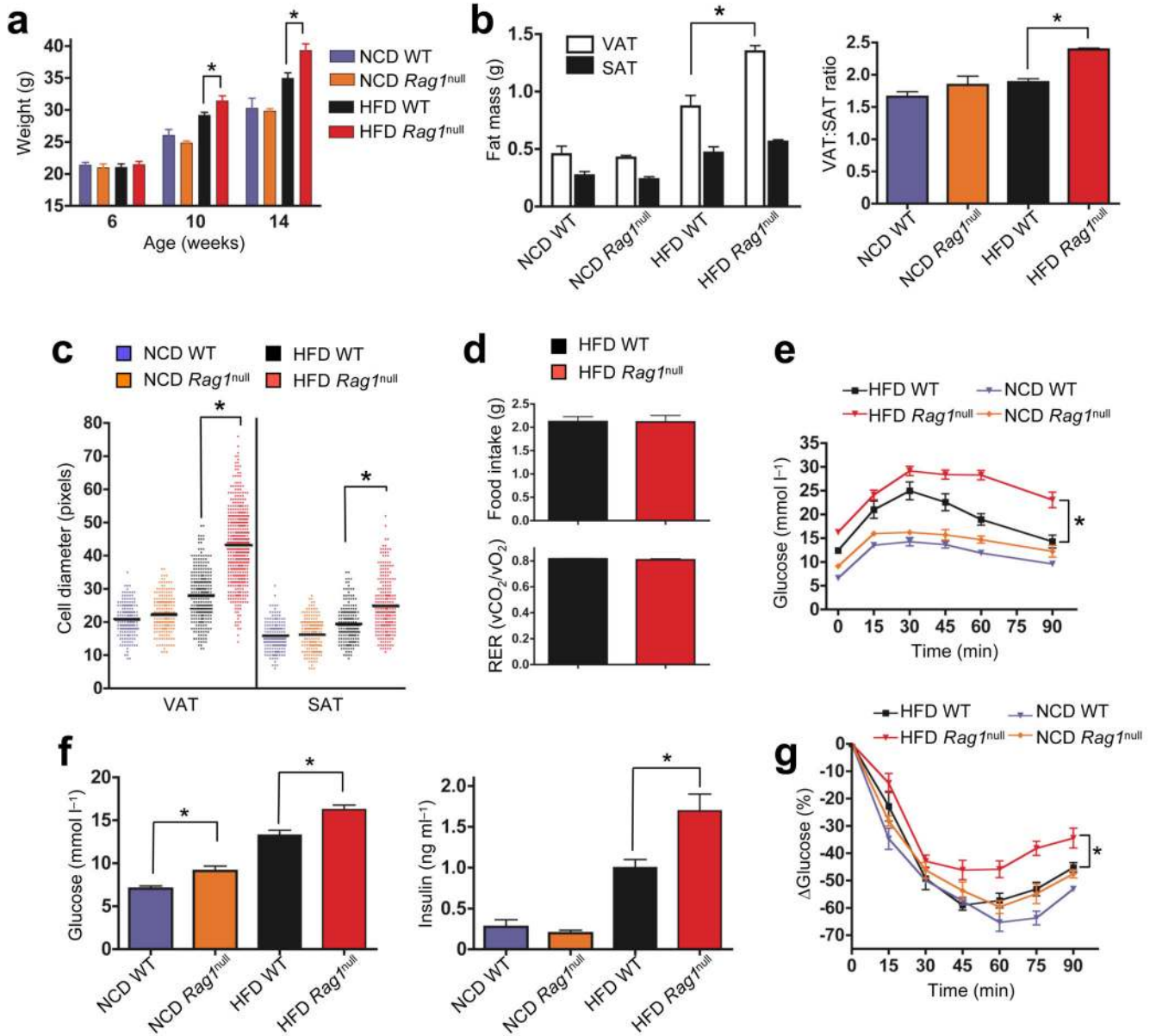
Figure 2. Impact of lymphocyte deficiency on weight gain, fat distribution, glucose tolerance and insulin resistance

a) Body weights of >6 wk old WT and RAG[null] B6 mice on NCD (n=20/group) or HFD (n=20/group, *p<0.03, Mann-Whitney, WT *vs.* RAG[null]). **b)** Weights of single epididymal VAT and inguinal SAT pads from 14–15 wk WT and RAG[null] mice on NCD or HFD (left panel: n=6 mice/group, *p<0.03, t-test), right panel: VAT:SAT ratio, *p<0.001, t-test. **c)** Relative fat cell diameter (see methods, n=3 mice/group, *p<0.0001, Mann-Whitney). **d)** Food intake (top panel) and respiratory exchange ratio (RER, bottom panel) in HFD WT or RAG[null] mice (n=4/group). **e)** Glucose tolerance of RAG[null] or WT mice on NCD or HFD (n=10/group, *p<0.02, 2-way ANOVA). **f)** Fasting glucose (left panel) or insulin blood levels (right panel) in 14 wk old HFD and NCD WT or RAG[null] mice (n=10 mice/group,

*p<0.05, t-test). **g)** Insulin tolerance test (ITT) in 14 wk old WT RAG^{null} mice on NCD or HFD (n=6–10/group, *p<0.05, two-way ANOVA).
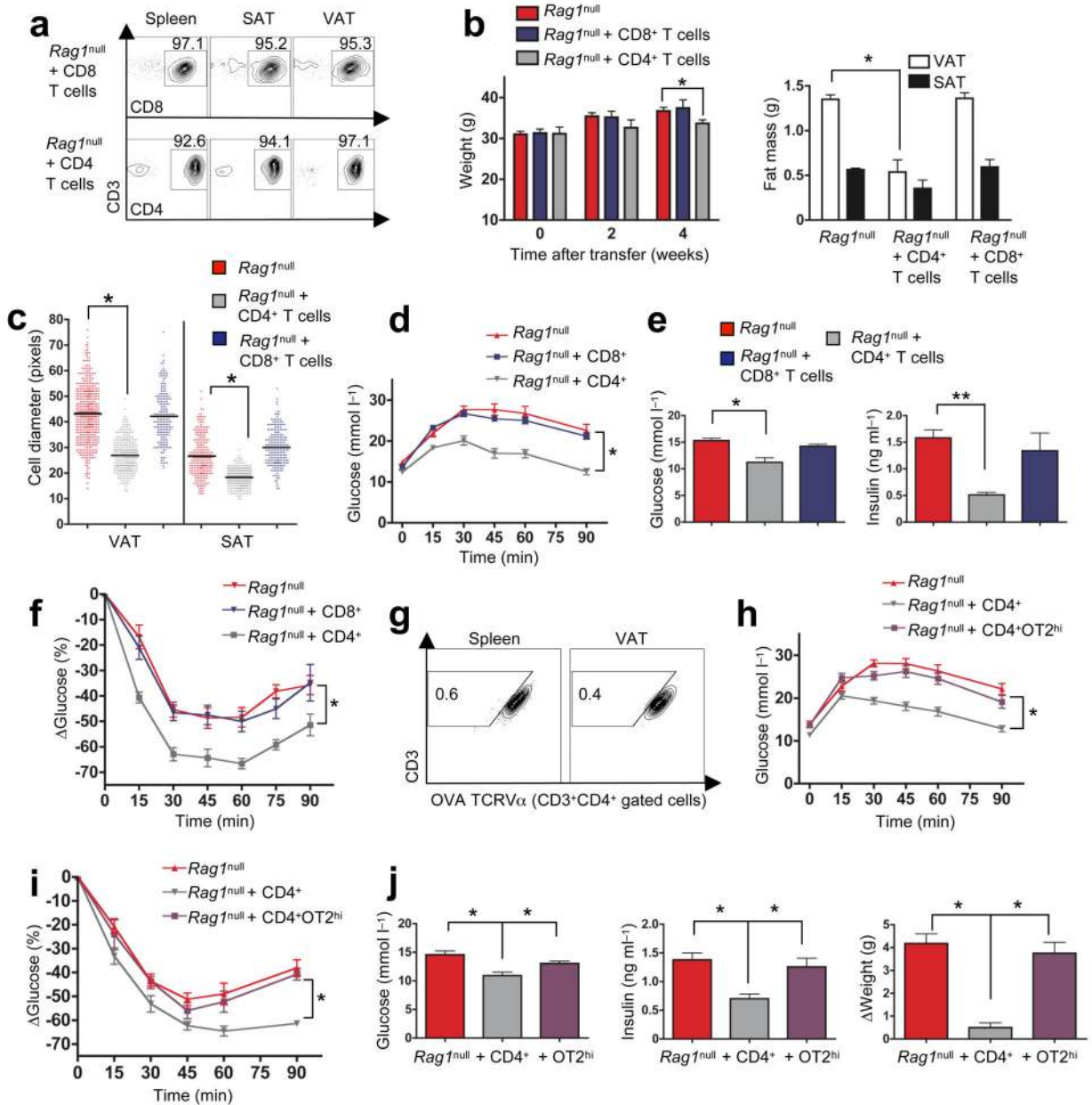
Figure 3. CD4+ T cell grafts reverse obesity-associated metabolic abnormalities in RAG[null] mice
a) FACS plots analyzing purity of CD3+CD8+ (top) and CD3+CD4+ (bottom) T cells in spleen, SAT, and VAT, 2 wk following transfer into 12 wk old HFD RAG[null] recipients. All subsequent experiments were performed 2–4 wk *post*-transfer and compared to non-transferred, age-matched, HFD RAG[null] mice. **b)** Left panel: body weights (n=5/group) of recipient mice were monitored post-transfer (*p<0.05, t-test, data from one of four similar experiments). Right panel: weights of individual VAT and SAT pads (n=5/group). CD4+ T cell transfer reduces VAT mass (*p<0.05, t-test). **c)** Adipocyte diameter following transfer of CD4+ or CD8+ T cells into HFD RAG[null] mice (n=3 mice/group, *p<0.01, Mann-Whitney). **d)** CD4+ T cell transfer improves glucose tolerance in HFD RAG[null] recipients (n=10/group, *p<0.0001, 2-way ANOVA). **e)** Fasting glucose (left panel) and insulin (right panel) in

CD4+ or CD8+ transferred HFD RAG^{null} mice (n=5–10 mice/group, *p<0.03, **P<0.01, t-test). **f)** HFD RAG^{null} mice reconstituted with CD4+ T-cells show improved insulin tolerance (n=10, *p<0.05, 2-way ANOVA). **g**) FACS plots of OT2 TCRVα re-rearrangements in spleen and VAT, 2 wk following transfer. The purity of CD4^{+}OT2^{hi} cells transferred was 99.5%. **h**) CD4+OT2:TCRα^{hi} (CD4^{+}OT2^{hi}) T cells fail to improve glucose and (**i**) insulin tolerance following transfer (n=5/group, *p<0.0001, 2-way ANOVA). **j**) Fasting glucose (left panel) and fasting insulin (middle panel) in CD4+ or CD4+OT2:TCRα^{hi} (OT2^{hi}) transferred HFD RAG^{null} mice (n=5 mice/group, *p<0.05, t-test). Right panel, CD4+OT2^{hi}:TCRα^{hi} T cells fail to improve weight post transfer (n=5 mice/group, *p<0.004, t-test).
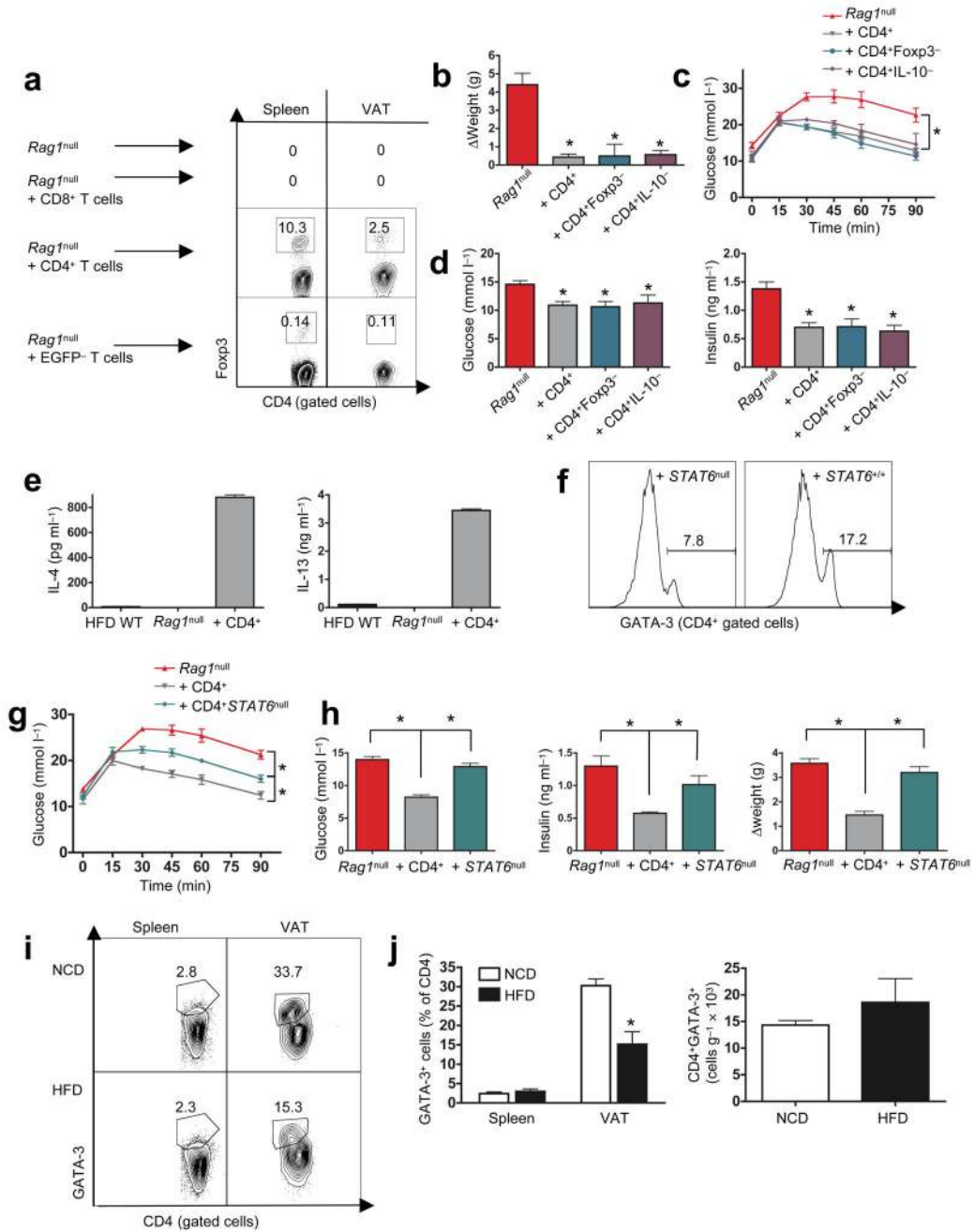
**Figure 4. CD4+Foxp3– T cells reverse metabolic abnormalities following transfer**

a) FACS plots of CD4+Foxp3+ T cells (%) in spleen and VAT, 3 wk after transfer of purified CD4+ or purified CD4+Foxp3– (EGFP[neg], 99.1% pure) cells, one of two similar plots shown. **b**) Change of HFD-RAG[null] body weight 3 wk *post* transfer of CD4+, CD4+Foxp3–, and CD4+IL-10[null] T cells (n=5/group, *p<0.01, t-test). **c**) GTT (n=5/group, *p<0.0001, 2-way ANOVA). **d**) fasting glucose (left panel, n=5 mice/group, *p<0.01, t-test) and fasting insulin (right panel, n=5 mice/group, *p<0.01, t-test), 3 wk *post* transfer of CD4+, CD4+Foxp3–, or CD4+IL-10[null] T cells into HFD-RAG[null] recipients. **e**) IL-4 (left panel) and IL-13 (right panel) produced by anti-CD3 *plus* anti-CD28 stimulated VAT T cells of 16

wk old HFD WT, and HFD RAG[null] recipients 3 wk *post* transfer of CD4+ T cells (n=3/group). **f**) FACS plots for CD4+ gated T cells from VAT of HFD RAG[null] mice that received either CD4+STAT6[null] (left panel) or CD4+WT (right panel) T cells 3 wk previously. **g**) Glucose tolerance 3 wk following transfer of CD4+ or CD4+STAT6[null] T cells (n=5/group, *p<0.05, 2-way ANOVA). **h**) Fasting glucose (left panel), fasting insulin (middle panel), and weight change (right panel) in HFD RAG[null] recipients 3 wk *post* transfer of purified CD4+ or CD4+STAT6[null] T cells (n=5 mice/group, *p<0.01, t-test). **i,** Left panel: representative FACS plot CD4+GATA-3+ (%Th2) cells in spleen and VAT of 14–16 wk old regular diet and HFD B6 mice. **j,** Left panel: pooled data from (i, n=4/group, *p<0.03, t-test), right panel: total number of CD4+GATA-3+ (Th2) T cells/g of VAT in regular diet and HFD B6 mice (n=4/group, p>0.4, t-test).
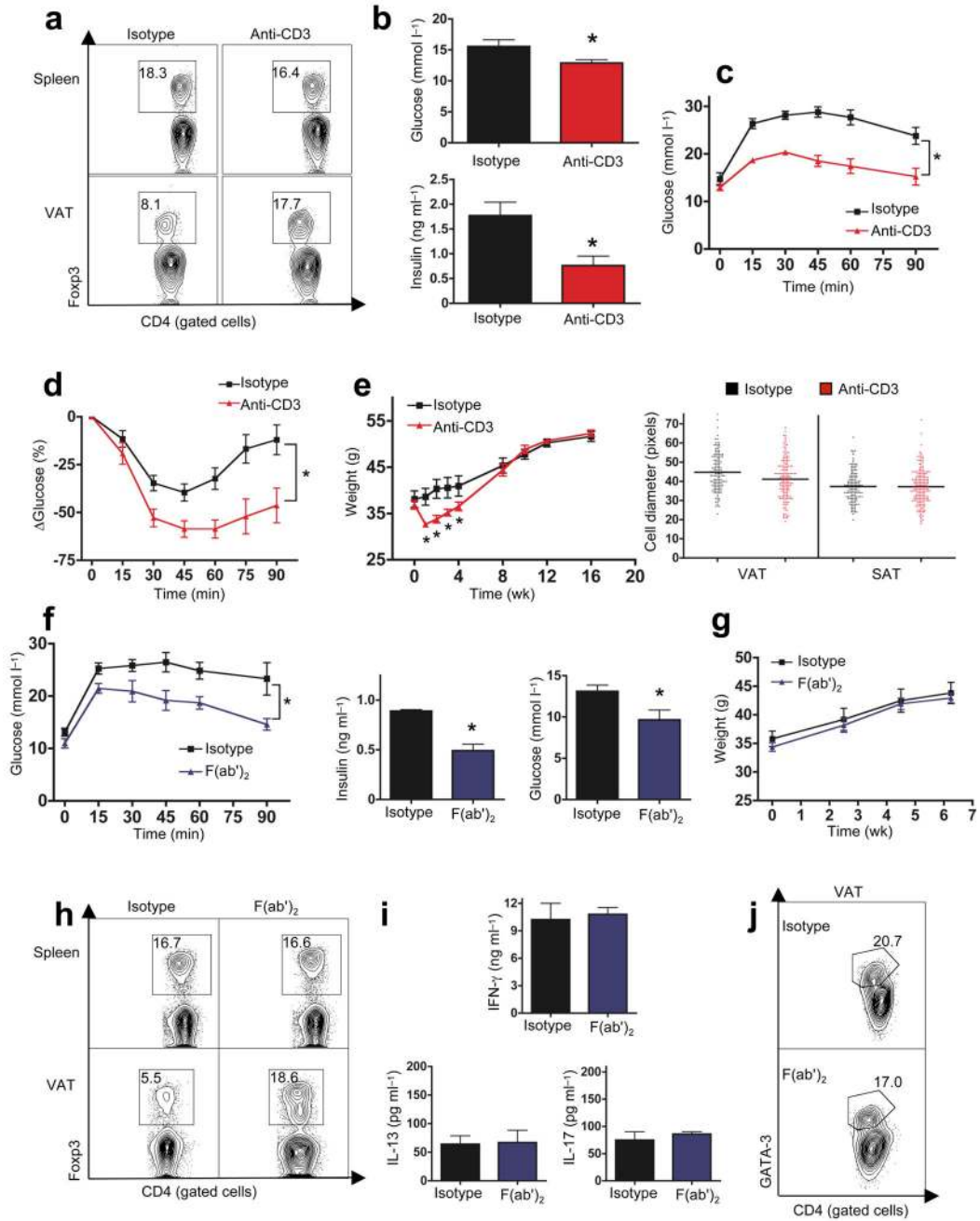
Figure 5. Anti-CD3 and its F(ab′)$_2$ fragment improve obesity-induced insulin resistance
16 wk old obese (HFD) B6 mice received anti-CD3 antibody (αCD3, **a–e**), Isotype-matched control IgG or anti-CD3-(F(ab′)$_2$ (**f–j**), maintaining HFD for 6 or 9 wk. **a.** FACS plots (%) of CD4+Foxp3+ Treg cells in spleen and VAT 9 weeks *post* αCD3 (one of 3 similar experiments shown). **b**) Fasting glucose (top panel) and insulin (bottom panel) after αCD3 (n=8, *p<0.05, t-test). **c**) Glucose tolerance (n=8, *p<0.0004, 2-way ANOVA) and **d**) ITT (n=8, *p<0.0005, 2-way ANOVA) *post* αCD3. **e**) Left panel: body weights of HFD mice following αCD3 (n=8, *p<0.05, t-test). Right panel: adipocyte diameter *post* αCD3 (n=3 mice/group). **f**) Glucose tolerance (left panel) 6 wk *post* F(ab′)$_2$ (n=5, *p<0.01, 2-way

ANOVA, one of 2 similar experiments). Fasting insulin (middle panel) and glucose (right panel) in HFD mice 6 wk following F(ab′)$_2$ (n=5, *p<0.04, t-test). **g**) Body weights of HFD mice following F(ab′)$_2$. **h**) CD4+Foxp3+ Treg cells in spleen and VAT of HFD B6 mice 6 wk *post* F(ab′)$_2$. (one of 3 similar experiments). **i**) IFNγ, IL-17, and IL-13, levels following stimulation of B6 VAT T cells with αCD3 *plus* anti-CD28, 8 wk *post* F(ab′)$_2$ (n=3/group). **j**) FACS plot of CD4+ gated, GATA-3 stained VAT T cells, 8 wk post F(ab′)$_2$).
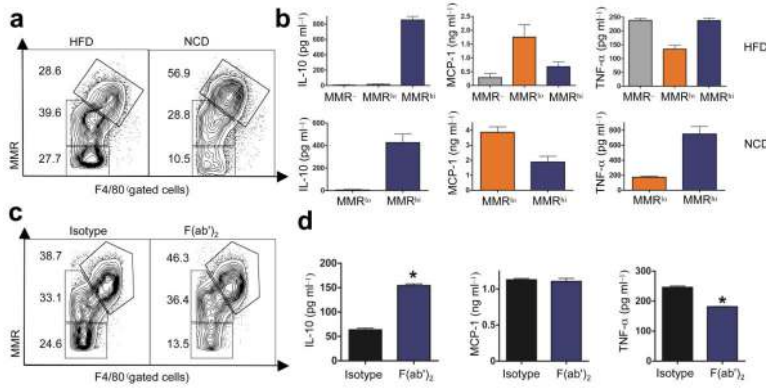
Figure 6. F(ab′)$_2$ therapy alters VAT resident macrophage phenotype

a) MMR^{hi} (%, upper gate), MMR^{lo} (middle gate), and MMR$^-$ (lower gate) macrophages from VAT of 16 wk old HFD or lean NCD B6 mice (representative data from 4 similar experiments). **b)** IL-10 (left panel), MCP-1 (middle panel) and TNFα (right panel) produced by LPS stimulated, F4/80+ macrophages sorted from VAT of HFD (top panel) or NCD (lower panel) mice into MMR$^-$, MMR^{lo}, and MMR^{hi} cell populations (one of 4 similar experiments). We consistently failed to obtain sufficient cell numbers for analysis of MMR$^-$ macrophages from VAT from lean mice. **c**) FACS plots from 2 independent experiments, measuring MMR expression in F4/80+ macrophages from HFD B6 VAT, 6 wk *post* F(ab′)$_2$. **d**) IL-10 (left panel), MCP-1 (middle panel) and TNFα (right panel) produced by LPS stimulated F4/80+ macrophages sorted from VAT 6 wk *post* F(ab′)$_2$ (n=3/group, *p<0.05, t-test).